International Journal of Remote Sensing
May 2010, Volume 31, Issue 15, pages 4069 - 4093
http://dx.doi.org/10.1080/01431160903199155

Mean seasonal cycle and evolution of the sea surface temperature from satellite and *in situ* data in the English Channel for the period 1986-2006

Bertrand Saulquin[a, *]; Francis Gohin[a]

[a] IFREMER, Dynamique des Ecosystèmes Côtiers, Plouzané, Brittany, France

*: Corresponding author : Bertrand Saulquin, email address : bsa@acri.fr

Abstract:

A night-time series of sea surface temperature (SST) of the advanced very high-resolution radiometer (AVHRR) sensors provided by the AVHRR/Pathfinder was analysed over the period 1986-2006 in the English Channel. The studied area is characterized by a strong influence of the bathymetry on the mixing of the water column, mostly through the action of the tide and waves, leading to regional patterns in the SST fields. Another specific aspect of the area is the relatively large number of *in situ* measurements available from coastal stations. The remotely sensed SST data with fine spatial resolution and high-frequency measurements made at coastal stations have been analysed using a common model. The long-term evolution of SST has been defined in this study through a linear trend while the seasonal evolution has been described through two harmonic functions. The daily satellite SST fields have been estimated over the period 1986-2006 by applying the kriging method to the anomalies calculated from the model. These interpolated temperatures were compared with *in situ* data, including many coastal stations unreachable at the sensor resolution. To use those coastal stations for comparison and to complement the satellite-derived data set, we defined transfer functions established from fine analysis of the *in situ* gradients along cross shore transects. The study showed the existence of a long-term warming and that this trend was not homogeneous in the area studied. The central part of the English Channel and the Western part of Brittany show an increase in temperature of about 0.6°C and the Northern part of the Irish and Baltic Sea, included in the studied area, show a maximum increase in the temperature of 1.6°C over the period 1986-2006.

1. Introduction

The spatial analysis of SST long time series, measured in situ or derived from remote sensing, has the potential to reveal local variations in the warming caused by the global climatic change. These features are particularly visible in coastal waters where the bathymetry strongly constrains the hydrodynamical circulation and gives a secondary role to the atmospheric variability. These long term changes in the patterns of the SST field will have significant consequences on the pelagic and benthic ecosystems. Some shifts are already observed in the benthic species, the seaweed and pelagic diversity, and spatial distribution (Scheffer, 2001). The relationship between SST changes and marine species variability is itself a high-priority research topic. The measurement of SST using the infrared channels of the AVHRR is now assumed to be accurate and the history of satellite-derived SST is discussed in an overview by McClain et al. (1985). The Pathfinder AVHRR data, available since 1985, used in combination with in situ data, offer a great potential in the comprehension of the global change pattern, especially if we consider that the warming caused by humans might be significant only since few decades. The main problem of the infra-red technique comes from its inability to provide SST estimations in the presence of clouds. For this reason many interpolation methods, making use of existing data in both time and space, have been developed in order to complete, as well as possible, pixels that are flagged due to cloud cover. Gandin (1963)

developed the optimum interpolation method (OI) as an analysis method for irregularly spaced data. The method used in this paper to perform the objective analysis of the historical data set is OI by kriging (Krige, 1951; Matheron, 1971) and the main goal of this study is to interpolate daily SST fields for the English Channel using AHRR/Pathfinder v5 data for the period 1986-2006. These daily SST fields will be used for comparison with an historical *in situ* data set to study the warming characteristics in the English Channel.

Global warming has been studied from satellite and *in situ* SST data for many years. Strong *et al.* (2000) characterized the global tendencies using 13 years of AVHRR SST data alone. Reynolds (2002) performed daily optimal interpolation of SST on the 1° spatial resolution grid of the National Oceanic and Atmospheric Administration (NOAA) to characterize the large scale warming from 1981 to present from blended *in situ*/satellite data. Casey and Cornillon (1999) built up an entirely satellite-based climatology which was particularly accurate compared to a first version provided by Reynolds (1995). In the recent years several climatologies were generated from satellite data. Amongst these climatologies we can mention those of Casey and Cornillon (2001), Faugères *et al.* (2001), and Armstrong and Vazquez-Cuervo (2001).

Despite their qualities, the practical use of these global climatologies for the monitoring of the coastal region is hampered by their resolution and eventually by the spatial smoothing applied by some of the methods. The effect of the resolution is particularly critical when you want to use the satellite data to complete an *in situ* data set obtained from a conventional coastal monitoring network in areas where SST gradients are very important. Recently, Mesias *et al.* (2007) derived a daily high resolution climatology on the Northwest Atlantic using the unique AVHRR 1km resolution data set of the Universisy of Rhode Island (URI), in an area where the meandering Gulf Stream current introduces some high frequency variability in the SST. In that case the high resolution of the sensor fits particularly the local hydrodynamical conditions. Unfortunately, these long time series of high resolution of AVHRR data, acquired in LAC (Local Area Coverage) mode, are not available everywhere. The second limitation inherent to any climatology is their static representation of a temporally bounded situation in a changing environment. This is particularly obvious when anomalies calculated from the two climatologies provided by Faugère *et al.* (2001) over the period 1985-1995, and by Casey *et al.* (2001) over a more recent period 1985-2001 are compared. These two climatologies are based on the same type of data (AVHRR Pathfinder), and the more recent climatology is the warmest because of the clear SST warming for the period 1995-2001.

Koutsikopoulos *et al.* (1998) had a specific approach that includes the temporal aspect of the SST trends. They derived the long term and seasonal characteristics of SST by using two harmonic components and a linear trend. Their study was performed using 10 day period SST fields provided by Meteo France and interpolated from *in situ* observations over the Bay of Biscay. For the period 1972-1993, they showed a mean warming of 0.064°C per year in the Bay of Biscay and a more intense warming, 1.4°C for the whole period, in the Southern-Eastern part of the Bay. Although the assumpted linear trend of the warming might be debated, we must admit that the temporal decomposition of the SST signal that they proposed is particularly suited for the representation of the local trends in temperature.

In this study we used the AVHRR Pathfinder v5 archive to investigate both the long term and the seasonal components of the SST variability. We derived, in a first step, the same SST model as Koutsikopoulos *et al.* using two long *in situ* time series available at Roscoff_Estacade and Flamanville.

In a second step, we used only the satellite data to derive the SST model at any point of a 5 km x 5 km grid. We considered, for both *in situ* and satellite data, the period 1986-2006 of our longest *in situ* time series. In a last step, once the parameters of the climatological SST model have been defined at any point, we considered that the daily anomaly, defined as the deviation between SST and the expected value provided by the model, was sufficiently stationary in a statistical sense to be analysed through the geostatistical techniques and interpolated by the kriging method (Gohin and Langlois, 1993). The interpolated daily SST field was obtained by addition of the kriged anomaly to the model output for that day, and the validation was performed using scientific cruises and monitoring network data available on the area for the period studied.

2. The data

2.1 In situ data

Two *in situ* temperature time series from 1986 to 2006 were firstly studied. The first is the biweekly time series of the Roscoff_Estacade station provided by the French coastal 'Réseau de surveillance du phytoplancton et des phytotoxynes' (REPHY) network, and the second is the daily time serie of the nuclear plant of Flamanville (Normandy) provided by Electricite De France (Luc Drévès, personal communication). The *in situ* SSTs for validation have been obtained from two sources, from French coastal monitoring networks and scientific cruises in the English Channel. Four selected transects data (composed of an offshore and a boundary coastal station), SRN_Dunkerque, Wimereux, SRN_Boulogne and Roscoff were obtained from the REPHY network, including the 'Suivi Régional des Nutriments' (SRN) network, and the 'Service d'Observation du Milieu Littoral' (SOMLIT) network managed by the French 'Institut National des Sciences de l'Univers' (INSU). For each transect, the offshore station has been used for direct comparisons between observed or kriged satellite-derived SST and *in situ* measurements. These offshore stations provide long time series of SST at location sufficiently distant from the coast to perform direct comparisons with satellite data while avoiding any land contamination. Finally the transects were used to study the temperature gradient near the shore and the possibility to estimate the coastal SST from the offshore one using a transfer function. The SST time series of the French 'Mesures Automatisées en Réseau pour l'Environnement et le Littoral' (MAREL) instrumented buoy located at Boulogne (Carnot) was also used to characterize the day/night variability. The mean characteristics of the selected stations are presented in Table 1 and their locations are shown in figure 1. Temperature is measured daily at Flamanville, every two weeks at Roscoff (high water in neap tide), Dunkerque, Wimereux and Boulogne (high water in spring tide), and every twenty minutes at MAREL_Carnot (but only since March 2004).

The second set of *in situ* data is composed of thermosalinograph data collected during scientific cruises for the same period. These data were extracted from the Coriolis database (http://www.coriolis.eu.org/) with nevertheless most of them collected in the recent years. Conversely to *in situ* data, the thermos-alinograph data have been filtered regarding a sampling time interval between 10 p.m and 10 a.m and they were filtered using the level 2 (probably good data) of the level quality flag. Only 9 profiles (CTD, XBT), filtered on the same manner, were available on this area for the period 1986-2006 and therefore were discarded.

Table 1. Selected stations and their mean characteristics. Positions of the stations are indicated on figure 1.

Station from north southwards	Observation period, number of observations	Sampling frequency	Data source	Characteristics
Point_3_SRN_ Dunkerque	January 1998 to December 2005, 63	Biweekly	REPHY/ SRN	Offshore station of the Dunkerque transect, located 6 km offshore
Point_1_SRN_ Dunkerque	January 1998 to December 2005, 69	Biweekly	REPHY/ SRN	Coastal station of the Dunkerque transect
Point_3_SRN_ Boulogne	January 2000 to December 2006, 109	Biweekly	REPHY/ SRN	Offshore station of the Boulogne transect, located 8 km offshore
Point_1_SRN_ Boulogne	January 2000 to December 2006, 118	Biweekly	REPHY/ SRN	Coastal station of the Boulogne transect
dMarel_Carnot	March 2004 to December 2006	20 min	SOMLIT/ IFREMER	Instrumented buoy close to the Boulogne harbour
Wimereux_L	Every 20 min November 1997 to December 2006, 111	Biweekly	SOMLIT	Offshore station of the Wimereux transect, located 10 km offshore
Wimereux_C	November 1997 to December 2006, 111	Biweekly	SOMLIT	Coastal station of the Wimereux transect
Flamanville	January 1986 to December 2006, 7670	Daily	EDF	The Flamanville station is located at the shore, near the power plant
Roscoff_Astan	January 1998 to December 2005, 51	Biweekly	SOMLIT	Offshore station of the Roscoff transect, located 5 km offshore
Roscoff_Estacade	January 1986 to December 2006, 455	Biweekly	SOMLIT	Coastal station of the Roscoff transect

2.2 Satellite data

Satellite SST data are extracted from the global AVHRR Pathfinder SST v5 daily product from 1986-2006 (http://podaac.jpl.nasa.gov/DATA_PRODUCT/SST/index.html). The AVHRR Oceans Pathfinder SST algorithm is based on the NLSST (Non-Linear SST) algorithm developed by Walton *et al.* (1998). The NLSST algorithm has the following form:

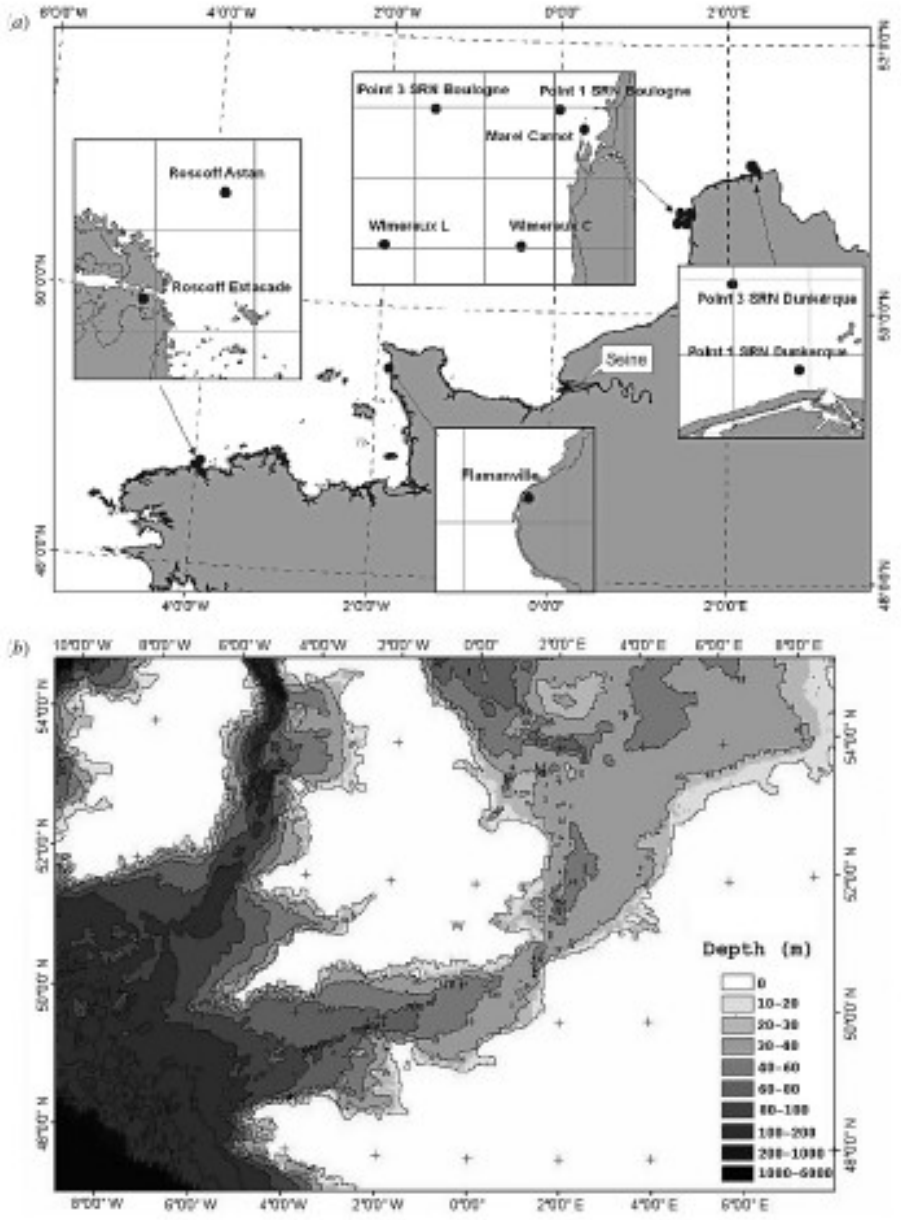

Figure 1. (*a*) Locations of the studied coastal stations and (*b*) Bathymetry on the area.

$$SST_{sat} = a + b\,T_4 + c\,(T_4 - T_5)\,SST_{guess} + d\,(T_4 - T_5)\,(\sec(\rho) - 1) \quad (1)$$

where SST_{sat} is the satellite-derived SST estimate, T_4 and T_5 are brightness temperatures in AVHRR channels 4 and 5 respectively, SST_{guess} is a first-guess SST value, and ρ is the satellite zenith angle. Coefficients a, b, c, and d are estimated from regression analyses using co-located *in situ* and satellite measurements (or "match-ups") for a certain period (generally on a month by month basis). In consequence, the satellite temperature, which is related to the « skin temperature » of the uppermost layer of the ocean and responsible for the IR emission, has been transformed to a « bulk » temperature by calibration to *in situ* temperature assumed to be measured at a depth of approximately one meter.

The platforms used in this data set are the NOAA-9, 11, 14, 16 and 17. These platforms perform two rotations a day, one descending at night with a node time around 2 AM for the 9, 11, 14, 16 and 10 AM for the 17, and one ascending 2 hours later. To reduce the diurnal effect we have selected only the descending orbits. A quality control was then performed by selecting pixels with a quality flag level greater than 3. This quality flag is provided in the Pathfinder v5.0 product, and its level was determined using Kilpatrick studies (Kilpatrick *et al.*, 2001). SST data were then projected onto a regular grid in longitude (0.075°) and latitude (0.05°) allowing a spatial resolution of about 5 km x 5 km. One condition for the utilisation of OI methods is that the data do not contain long-term biases. We assumed in this paper that existing biases between the AVHRR sensors have been corrected in the AVHRR Pathfinder v5 product. Therefore, no correction or inter calibration between the AVHRR sensors has been done.

3. The theoretical model

3.1 The formulation of the mean SST cycle and the linear long-term trend

The model was calculated using the two long time series of Flamanville and Roscoff and also at any location on the English Channel using the satellite data. SST is modelled by the equation:

$$T=P_0+P_1 t-P_2\cos(2\pi/365.25*(P_3+t))-P_4\cos(2\pi/182.625*(P_5+t)) \quad (2)$$

Where T is the sea surface temperature, t the number of days since the 01/01/1986. P_0 + P1*365.25/2 can be interpreted as the mean temperature of the first year of the period studied (1986) and P_1 is the slope of the linear warming. The amplitude P_2 corresponds to the half-difference between the coldest and the warmest temperature of the year and the phase P_3 corresponds approximately to the coldest day in the year (considering the negative sign before the first harmonic). The amplitude of the second harmonic P_4 is very low and this second harmonic contributes to the formation of the two plateaus reached by the temperature in winter and summer and the expression of the rapid temperature changes in spring and autumn. P5 is the phase of the second harmonic and at this stage it is difficult to give a physical meaning to that parameter.

The parameters are estimated using an iterative process to minimize the residuals between the observations (*in situ* data at Flamanville and Roscoff or satellite data for the whole area), and the temperatures derived from the model. After the estimation of the parameters of the equation (2) we can define a first-guess SST at any day and any location. The deviation observed between the AVHRR image of the day and the first guess will be considered as the daily anomaly.

3.2 The kriging method for interpolation

The parameter which will be estimated by kriging is the anomaly. Each day, the SST anomaly A_{SST} at each pixel centred on x_0 and at t_0 will be interpolated using the n satellite data $A_{SST}(x_i,t_i)$ available in the space-time vicinity of (x_0,t_0)

$$A_{SST}(x_o,t_o)=\sum_{i=1}^{n}\lambda_i A_{SST}(x_i,t_i) \quad (3)$$

λi are the weights given to the observed anomalies $A_{SST}(x_i,t_i)$.

For ensuring a well balanced set of observations, in space and time, the data used to calculate the estimation or control points, are sought using a procedure that scrutinizes carefully the anomaly images in the vicinity. The research procedure describes decreasing disk in space, starting with the largest disk for the current day, and then alternates between previous and following days. Once the anomaly has been estimated it is added to the mean SST at location (x_0, t_0), derived from formula (2), to obtain the SST.

The Semi-variogram

Determining the weights λ_i in equation (3) is the main issue in optimal interpolation. In geostatistics, it is assumed that because the SST anomaly (A_{SST}) is a random process characterised by stationary properties, the variance of the estimation error (V_K) can be expressed using the function structure or the covariance obtained through the structural analysis.

$$V_K = VAR\left[A_{SST}(x_o,t_o) - \sum_{i=1}^{n} \lambda_i * A_{SST}(x_i,t_i) \right] \quad (4)$$

The so-called *simple kriging* assumption is that, at a position x and a distance h from that position, the mean of the increments $[A_{SST}(x+h) - A_{SST}(x)]$ is zero and the covariance (or the semi-variogram of the increments) of A_{SST} is known. The kriging estimator is the one that minimizes the variance of the estimation error. The hypothesis and the derivation of the estimation error is very similar in simple kriging to the technique applied by Bretherton *et al.* (1978) and well known in the oceanographic literature.

The semi-variogram (or the structure function), γ, is expressed for each lag of time dt (from dt = 0 to dt = 4) using the equation (5) for the n(h) points separated from the distance h.

$$\gamma(h) = (1/2n(h)) \sum_{i=1}^{n(h)} [A_{SST}(x+h) - A_{SST}(x)]^2 \quad (5)$$

In the simple kriging hypothesis where the mean of increments is zero and the semi-variogram exists, the variance of kriging can be developed as:

$$V_K = -\sum_{i=1}^{n}\sum_{j=1}^{n} \lambda_i * \lambda_j \gamma(x_i,t_i;x_j,t_j) + 2\sum_{i=1}^{n} \lambda_i \gamma(x_i,t_i;x_o,t_o) \quad (6)$$

Assuming that their sum is equal to 1 (insuring no bias), the coefficients λ_i are solution of the kriging system if they minimize the variance V_K. This is obtained by setting all the partial derivatives, relatively to λ_i, to 0. By doing this, we get a n+1 linear system (7) with λ_i and μ, a Lagrange coefficient accounting for the non bias constraint, as unknown values.
For the λ_i solution of the kriging system it is shown that

$$V_K = \sum_{i=1}^{n} \lambda_i \gamma(x_i,t_i;x_o,t_o) - \mu \quad (7)$$

4. Results

4.1 The mean SST cycle and the linear long-term trend at Roscoff_Estacade and Flamanville

The formulation (2) fits well the observed *in situ* SST at Flamanville and Roscoff (figure 2a and 2b). We have tested a first formulation of the SST without the second harmonic, thus keeping the constant and the first harmonic. This first formulation explained 93% of the total variance at Flamanville and 89% at Roscoff. As shown by the autocorrelation diagram of the residual (figure 3a), there were still another cyclic component with a period of 6 months. This second harmonic explained only 3% of the variance of the original temperature time series at both stations of Flamanville and Roscoff, and after the removal of this second harmonic, no cyclic signal could be observed. The yearly pace at Flamanville is 0.073 °C per year and 0.007 °C per year at Roscoff over the period. This difference illustrates the role of the local hydrodynamic conditions on the observed warming of the water masses. The use of satellite data to derive the same SST temporal model will confirm the presumption of non uniform warming in the English Channel and the importance of the local physical and hydrodynamic properties on that process.

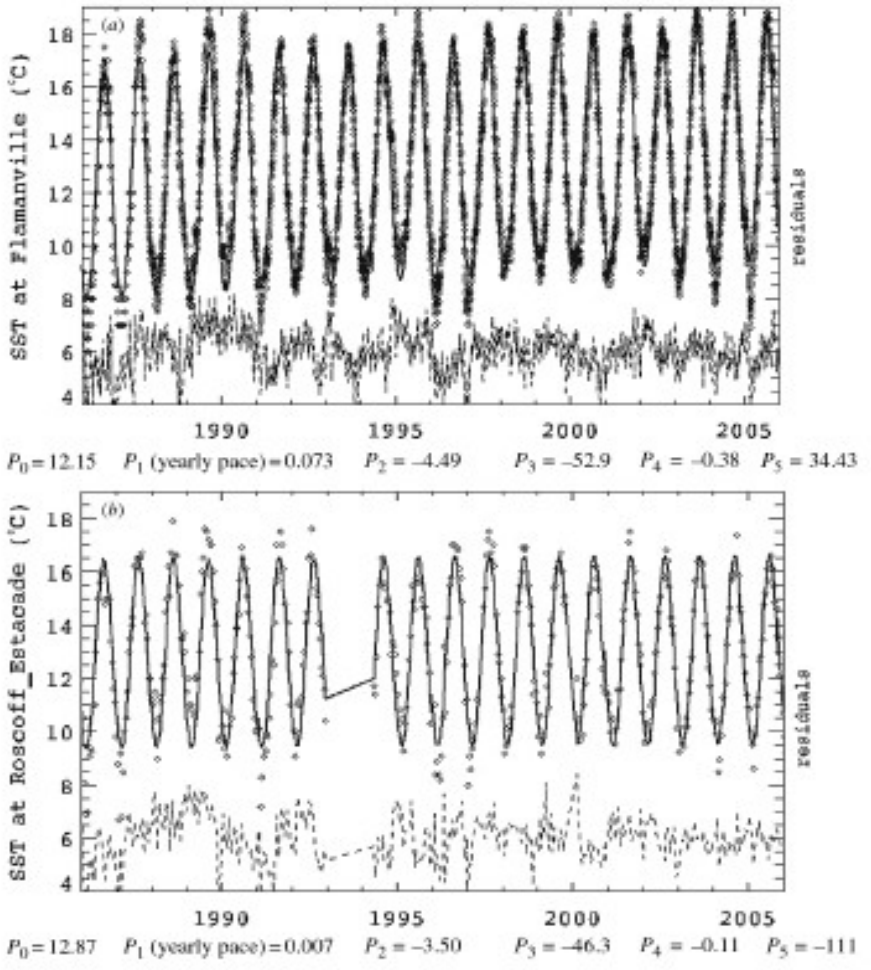

Figure 2. Seasonal time series at (*a*) Flamanville and (*b*) Roscoff_Estacade.

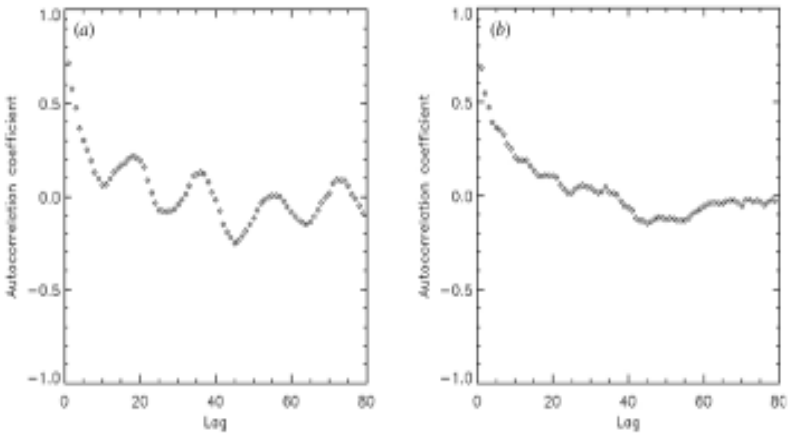

Figure 3. (*a*) Autocorrelogram of the remaining residuals at Flamanville after extraction of the linear trend and the first harmonic and (*b*) extraction of the linear trend and the two harmonics. A lag is a 10-day period.

4.2 The mean SST cycle and the linear long-term trend on the satellite grid

We used Pathfinder satellite time series to derive the SST model on a 5 km x 5 km grid using the same iterative process and temperature model defined in equation (2). For each point of the grid, each parameter of the model is calculated (figure 4a-f). A minimum of 400 retrievals for the satellite data has been used for the period 1986-2006 to calculate the parameters of the model. Below that threshold the parameters are not calculated, and the boundary coastal pixels where satellite retrievals are very poor are coloured in black corresponding to no data. The mean SST parameter (P_0) showed a distribution of the temperature equivalent to what was observed on the mean of 1986 extracted from the Pathfinder year product (not shown), with a Southern gradient of temperatures. Temperature range for the mean temperature in 1986 is between 9°C in the Northwest part on England and 13.5°C in the South of Brittany (figure 4a).

The parameter P_1, corresponding to the warming slope, showed a lower warming rate in the middle of the English Channel (0.04°C/year) and the West Southern area of the French Brittany. The first boundary corresponds to the Ushant front and its extension toward the North, and the second to the Iroise Front (figure 4b). These fronts underlie the boundaries between the very well mixed water masses by the tide of the Eastern part and the deepest Western areas where the stratification is more significant. The tide influence on the warming appears also on the French coasts, where a gradient of 0.02°C/year is observed between P_1 pixel values at the shore and 10 km (2 pixels) offshore. In the Irish Sea and the North Eastern part of England, the warming is more important with some values of 0.075°C/year.

The parameter P_2 corresponds to the yearly cycle SST amplitude. P_2 is between 2.5 and 7.5°C. Values of P_2 are partially linked to the bathymetry (figure 1b) and the stratification of the water column, with higher values for shallow stratified areas of the North Western part (<20m) and lower values for the Irish Sea and the West offshore area of Brittany where the water column is well mixed.

The Parameter P_3 appears to be linked to the turbulence. Coldest days are reached lately in the year in high turbulent areas like the middle of the English Channel, where the bathymetry is between 20 and 80 meters, and in the Irish Sea with characterised by deeper but very turbulent waters. The shallow coastal

waters are quickly influenced by atmospheric cooling and the coldest days are observed around the day 40 on the Belgium shores to the day 75 in the middle of the Irish Sea.

The Parameter P_4, the amplitude of the second harmonic, is between 0 and 1.5°C and shows a Westward gradient in the middle of the English Channel and South-Western gradient in the Irish Sea. It seems to be correlated with the turbulence. This means that the plateau characterizing the minimum of SST in winter and its maximum in summer are limited in time for the Eastern part of the English Channel and in the Northern part of the Irish Sea.

No clear feature is apparent for the parameter P_5.

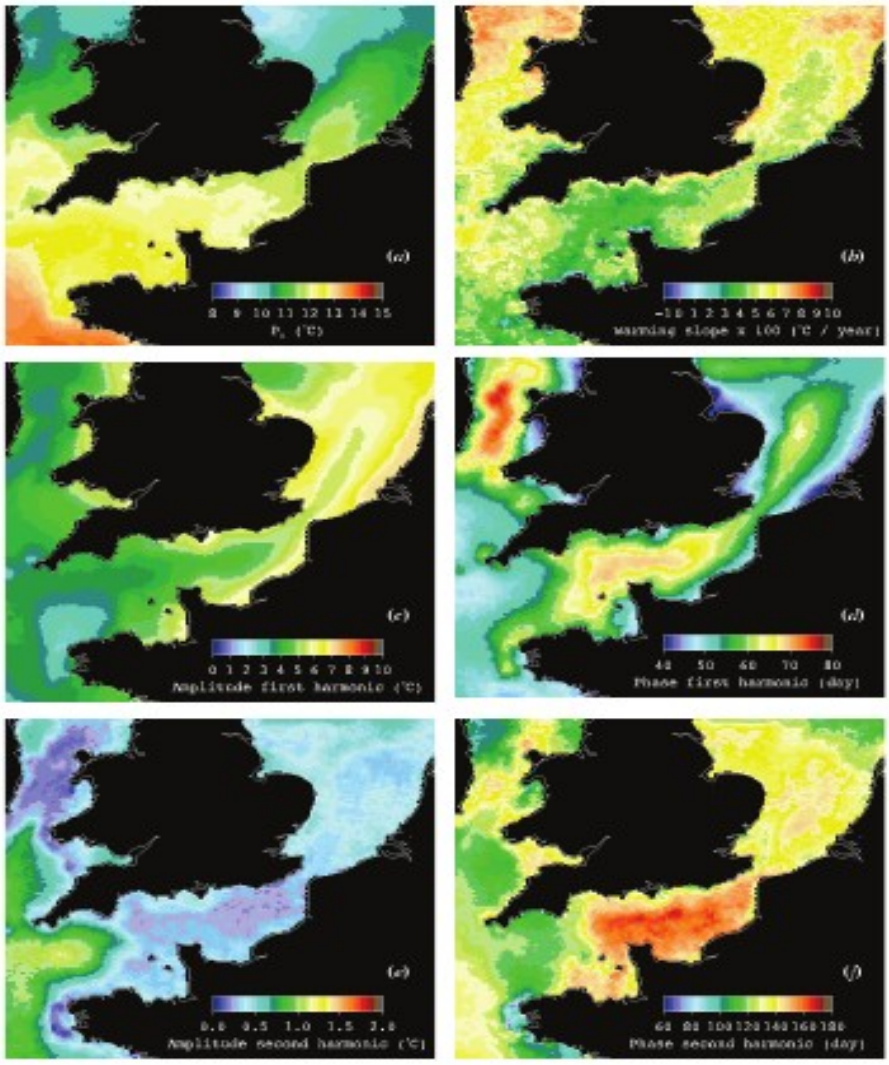

Figure 4. Parameters of the seasonal time series derived using AVHRR data from 1986 to 2006. (*a*) P_0, the mean temperature in 1986, (*b*) P_1, the warming slope, (*c*) P_2, the amplitude of the first harmonic (yearly period), (*d*) P_3, the phase of the first harmonic, (*e*) P_4, the amplitude of the second harmonic (6-month period), (*f*) P_5, the phase of the second harmonic.

The standard deviation of the residuals (STD) of the satellite data compared to the model (figure 5a) shows that the largest residual variations occur in the Northeast part of the studied area, where shallow waters result in high temperature amplitude between summer and winter. The minimum observed in the residuals STD occurs in the very well mixed areas, in the North of the Irish Sea, the middle of the English Channel and the Northwest shore of the Brittany. The explained variance (EV) map (figure 5b) shows that our temperature model explained a large part of the satellite SST variability over the whole area, where the temperature variations are dominated by a seasonal heating cycle. We can however notice that the EV decreases to 80% for the two areas of the Iroise Front and the beginning of the Ushant front.

The effect of the calculated long linear trend is revealed by the difference between the mean SST derived from the model for the years 1986 (figure 6a) and 2006 (figure 6b). We observe over this period a warming between 0.5°C in the Southern part of the area and the middle of the English Channel and 1.5°C in the Northern part . These observations are directly correlated to the local warming slope.

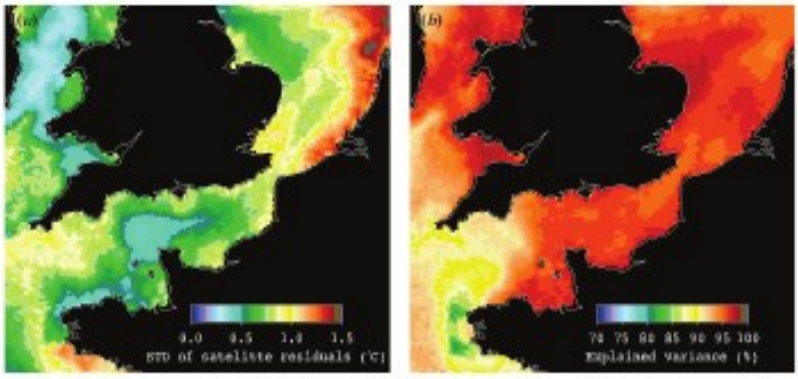

Figure 5. (*a*) Standard deviation (STD) of the satellite residuals from the model for the period 1986–2006 and (*b*) Variance explained by the model of the satellite data.

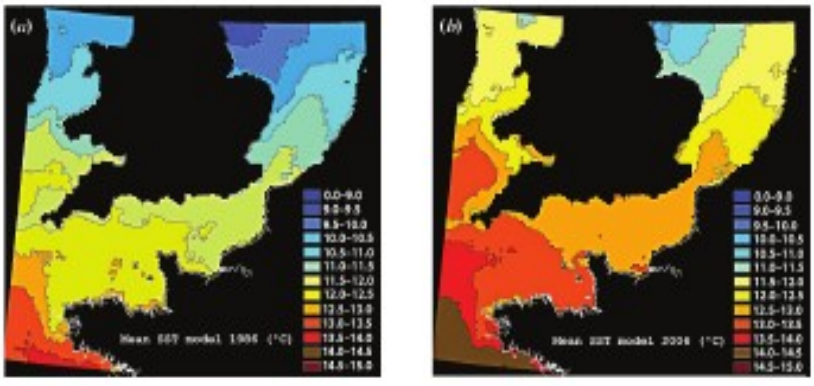

Figure 6. Means SST derived from the SST model for (*a*) 1986 and (*b*) 2006.

4.3 Interpolating the satellite SST by kriging

The semi-variograms

The theoretical semi-variogram is adjusted to the experimental semi-variograms (5) obtained from the semi-variance calculated in time and space. The following exponential function has been adjusted using the least square method**:**

$$\gamma(h,dt) = a(1 - \exp(-bdt - cdx)) + p_x + p_t \quad (8)$$

a+pt+px is the maximum observed variance (i.e. the variance of a sample where points are separated by a very large distance). b is the temporal factor of the semi-variogram. c is the spatial factor of the semi-variogram. Figure 7a-d shows the experimental semi-variograms, calculated for the whole area over the period 2000-2005, for dt = 0 day to dt = 4 days using (5) and the theoretical semi-variogram adjusted (8). px and pt appear as discontinuities at the origins of the semi-variograms for dt = 0 and dx = 0 respectively, and correspond to the purely random part of the SST anomaly at the scale of the observations. px is called the spatial nugget effect and corresponds to the variance due to the instrumental noise and the cloud residual effect *i.e.* the difference observed between two temperatures at very short distance (one pixel) at the same time. pt is the temporal nugget and corresponds to the temperature difference in a short time (dt = 1) for the same location. In practice pt could be mainly attributed to variation in the atmospheric corrections deriving, for instance, from two different zenithal angles of observations. For dt = 0, the semi-variogram of figure7.a reaches a threshold of 0.3°C² for dx = 400 km. Beyond this distance the covariance between two observations is null. Although this maximum distance could be used in open sea to seek the satellite observations for dt = 0, we chose a distance of 150 km, more dedicated to the interpolation in coastal areas where the gradients are more important. The timespan of 9 days (4 days before and 4 days after the current day) was chosen as the semi-variogram γ (h,5) was almost flat *i.e.* the covariance between the observed anomalies was negligible for any distance.

Kriging the daily anomaly fields and derive the interpolated temperatures in the English Channel

Daily anomaly fields have been estimated for the whole area and the period considered, using the adjusted semi-variogram (8) and the observations within a spatio-temporal neighbourhood of nine days (four days before and four days after) and 150 km around the nodes of the kriging grid (figure 8). Each interpolated daily SST field has been then calculated by the addition of the kriged anomaly to the daily SST model output. A first kriging attempt with the nuggets adjusted in equation (8) resulted in discontinuities in the vicinity of clouds. Satellite SST affected by cloud are relatively scarce compared to the large set of clear and high quality values and their effect was not visible in the calculation of the empirical semi-variograms. However they have dramatic consequences in some situations, introducing visible artefacts in the interpolated SST fields. In order to prevent any strong local variability in the interpolated SST due to cloud-contaminated pixels in the neighbourhood, the temporal nugget px and the spatial nugget pt (which are in our hypotheses the variance of the purely random parts of the SST anomaly) have been considerably increased in the kriging system.. The initial observed values of 0.01 and 0.03°C^2 were adjusted respectively to 0.1 and 0.2°C^2. The coefficients of the theoretical variogram (8) obtained from the minimization of the residuals were a = 0.28, b = 0.2, and c = 0.009. There is also another aspect of the empirical semi-variogram that leads us to consider it as only an approximation of

the spatial variance of the SST. As a matter of fact the semi-variogram is calculated from pairs of satellite data obtained at night. For that reason the semi-variogram is unable to represent the diurnal variation that is observed in the *in situ* measurements. Nevertheless, the consequence of increasing the nugget values on the kriging error will be objectively assessed through a comparison with observed *in situ* SST.

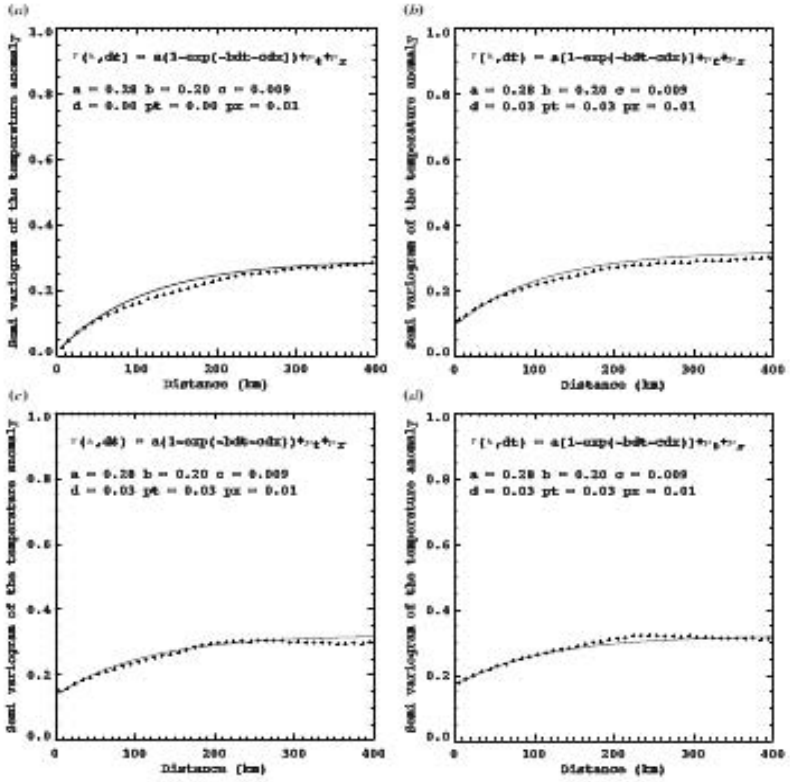

Figure 7. Semi-variograms of the temperature anomaly from the model, (*a*) dr = 0, (*b*) dr = 1, (*c*) dr = 2 and (*d*) dr = 3.

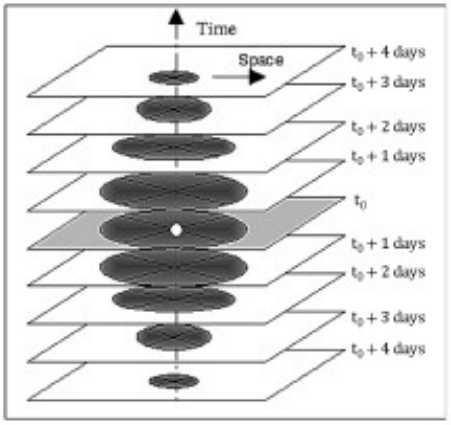

Figure 8. Method for seeking the control point dataset. The white dot represents the location of the temperature anomaly to estimate.

4.4 Satellite-derived SST compared to in situ observations

Figure 9a shows the scatterplots between satellite SST (direct or kriged) and thermosalinograph data, obtained from cruises. Figures 9b-e show the scatterplots of the satellite and *in situ* SST for the 4 selected offshore stations. These stations are sufficiently distant from the shore to perform direct comparisons with satellite data. The statistical results of these comparisons are shown in the table 2 for the cruises data and table 3 for the network stations. There is a constant negative bias of the satellite data. This bias compared to the thermosalinograph data is -0.17 °C for both kriged and direct satellite data and the standard deviation is 0.46°C for the satellite data and interpolated data. In comparison and to illustrate the impact of the nugget change we obtained, using the thermosalinograph data and the initial values for the nuggets, a bias of –0.18°C and a standard deviation of 0.49°C. These values are slightly higher to those observed after the increasing of the nuggets. The increase of the nuggets can smooth some observed structures and therefore degrade the interpolated SST, but it also mitigates the influence of the cloud-contaminated pixels that introduce high variability in the interpolated images. This bias is more negative for the selected coastal stations. This was expected as the satellite SST are night temperatures and the *in situ* measurements are made in the day. At the selected coastal stations, the satellite-*in situ* bias is of the order of -0.3°C which is quite compatible with the variability of the diurnal cycle (Brisson *et al.*, 2002). As expected, the bias observed on the kriged temperature is similar to that observed from the direct measurements. The kriging estimator is unbiased. The number of match-ups obtained with the thermosalinograph data is considerably increased, from 2057 to 11286, when considering the kriged temperature. The standard deviation is the same, 0.46°C, for both kriged and non kriged data, confirming the quality of the interpolation. In fact most of the standard deviation is likely to be due to the diurnal cycle and not to the interpolation.

Although the sampling time at the network stations occurs during the day, the data are used for direct comparison with the night satellite data (figure 9b-e). The bias satellite–*in situ* is negative for all the stations and its value is included between -0.1°C at Roscoff and -0.43°C at Boulogne. The standard deviation is between 0.4°C at Wimereux and 0.9°C at Boulogne, similar for both kriged and non kriged data. Figure 10 shows the diurnal cycle of surface SST at the MAREL instrumented buoy in the Boulogne harbour. Temperatures are coldest at the end of the night, at about 6 hours, particularly in summer

If we look at the SST of 2006 at Wimereux (figure 11a) we can observe that the kriged estimations are clearly close to the annual cycle of the *in situ* data. The smoothing effect leads to attenuate some high frequency variations observed in the satellite SST. The estimated error provided by the kriging procedure is in good agreement with the deviation observed between the kriged satellite and the *in situ* data at Wimereux for the year 2006.

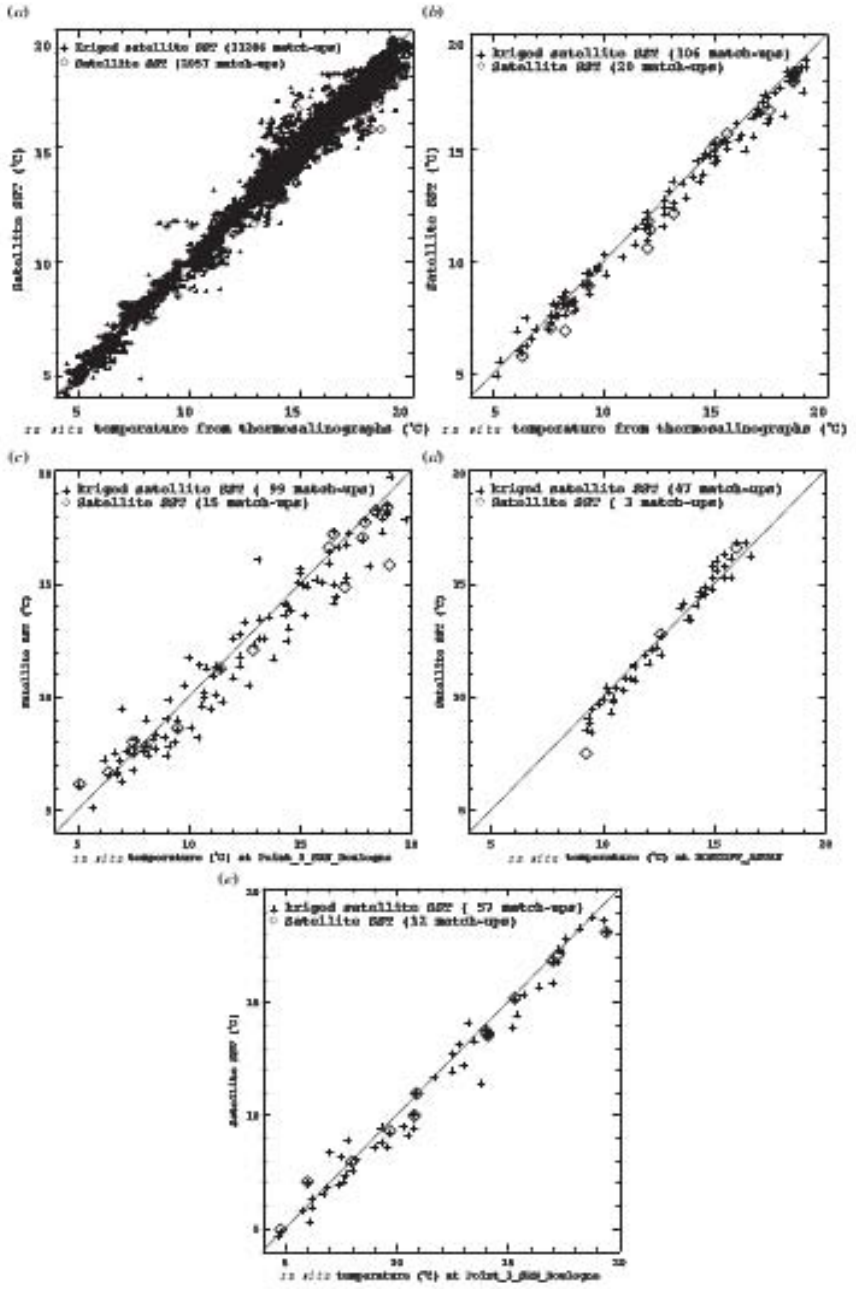

Figure 9. Satellite versus *in situ* scatter plots. (*a*) *In situ* data from cruises thermosalinographs, (*b*) *in situ* data at Wimereux_L, (*c*) Boulogne_3, (*d*) Roscoff_Astan, (*e*) Dunkerque_3.

Table 2. Satellite to cruise data comparisons. STD, standard deviation.

	Satellite SST			Kriged satellite SST		
Station	No. of match-ups	Satellite-*in situ* bias	Satellite STD	No. of match-ups	Satellite-*in situ* bias	Satellite STD
Thermosalinograph data	2057	−0.17	0.46	11 286	−0.17	0.46

Table 3. Satellite-to-offshore station data comparisons.

	Satellite SST			Kriged satellite SST		
Station	No. of match-ups	Satellite-*in situ* bias	Satellite STD	No. of match-ups	Satellite-*in situ* bias	Satellite STD
Wimereux_L	20	−0.47	0.43	106	−0.29	0.44
Point_3_SRN_Boulogne	16	−0.2	0.78	103	−0.43	0.98
Roscoff_Astan	3	−0.34	1.23	45	−0.1	0.49
Point_3_SRN_Dunkerque	12	−0.23	0.57	57	−0.32	0.64

4.5 Extrapolating the satellite SST at the coastal network stations

The coastal location of the stations of Roscoff_Estacade, Wimereux_C and Flamanville makes the extrapolation of the SST impossible from the estimated satellite anomaly alone. Even if the Pathfinder v5 provides some retrievals at the shore for the period 1986-2006, their quality level is often too low, due to the utilisation of a reference SST field which can dramatically differ at the shore, and the remaining data are too scarce to calculate the parameters of the model at these locations. It is therefore interesting to try to connect the coastal anomaly to the anomaly observed few kilometres offshore. The SST difference between two monitoring stations, Wimereux_L (offshore) and Wimereux_C is shown on figure 12a. Wimereux_L is 8 km offshore from Wimereux_C and the offshore minus coastal temperature difference is 1°C in February and -1°C in August. Therefore, we have considered a simple cosine (9) function to characterize the temperature difference (ΔT).

$$\Delta T = \cos((2\pi / 365.25)d) \quad (9)$$

d is the day in the year.

This function is then added to the kriged values at Wimereux_L and compared to the *in situ* data at Wimereux_C (figure 12b). Doing so, we observed (table 4) a good correction at the coastal stations of Wimereux_C and Roscoff_Estacade and the kriged data showed a bias of respectively -0.12°C and -0.19°C and a standard deviation of 0.56°C and 0.7°C for the entire period. Figure 12c shows an example for Wimereux_C. The correction in its actual form is less accurate at Boulogne_1 and Dunkerque_1 with some observed biases of -0.44°C and -0.39°C compared to the biases of -0.2°C and -0.23°C for Boulogne_3 and Dunkerque_3. This shows that the transfer function at these locations must be studied in more details.

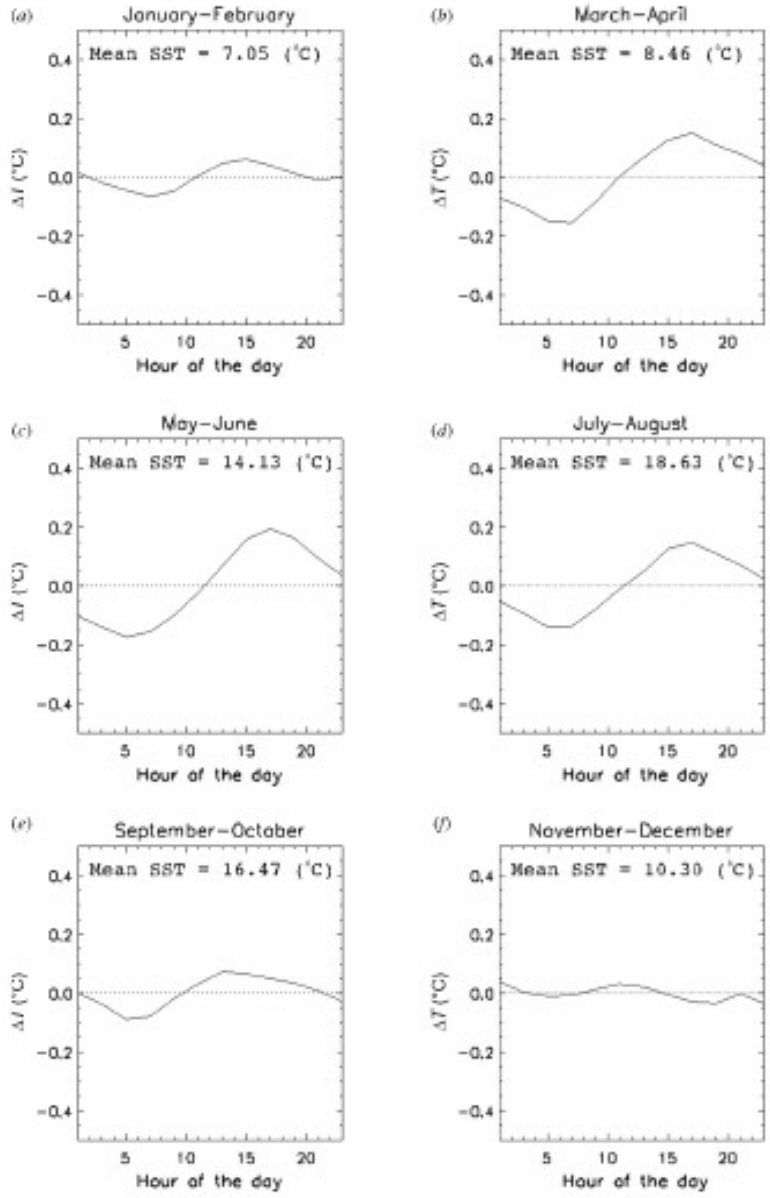

Figure 10. Daily temperature cycle (ΔT) at the Carnot Buoy throughout the year.

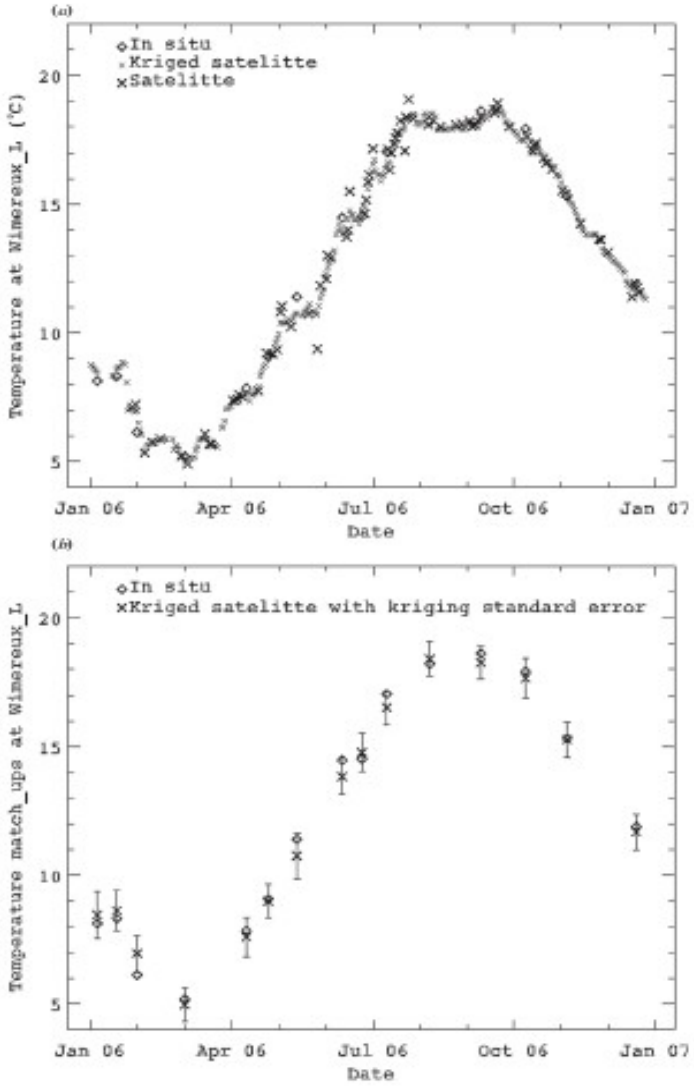

Figure 11. (*a*) Temperature cycle at Wimereux_L for the year 2006 and (*b*) Kriging error estimation on match-ups at Wimereux_L for the year 2006.

5. Discussion

Our model of the SST variability, expressed as a linear temporal trend and two harmonic functions, implies a regular warming and an identical shape for the SST seasonal curve at any location. In their study on the Western North Atlantic Ocean, Mesias *et al.* (2007) tested the number of significant harmonics at any location. In most of the cases, their automatic procedure recognized 3 harmonics as significant in their area of high SST variability. Our hypothesis of two harmonics is more restrictive, but tested on satellite and in situ data, it proved to fit very well the seasonal variability of the SST in the English Channel, with more than 95% of the variance explained in most of the cases. Figure 5.b shows that only two frontal areas (Ushant and Iroise) are explained with a score inferior to 85% of the initial variance. In these areas, the location of the front moves in relation with tide and winds at such an high frequency that many more harmonics would be necessary to describe the variability. The choice of two harmonic functions, limiting the number of parameters in the model, gives also more robustness to our

calculation of the warming coefficient which is certainly the most questionable part of our hypothesis. Figure 4b shows a clear gradient of the linear warming Northwards. The observed warming rates are between 0.03°C per year near Brittany and 0.075°C per year on the North of the Irish Sea and the North Sea. This represents a temperature increases over 21 years of 0.63°C and 1.6°C that could have impacted the ecosystem. This warming can be attributed to a large number of factors (air temperature, wind, water depth, turbulence) that we cannot develop here. However we can evaluate the relation between the local variability of the SST in the studied area and the North Atlantic Oscillation (NAO) through an analysis of the correlation between the NAO coefficient and the deviation from our model. Figures 13a-b show the variation of SST and the NAO index in wintertime (January and February) at Roscoff and Flamanville stations. NAO index data has been provided by Tim Osborn at http://www.cru.uea.ac.uk/~timo/projpages/nao_update.htm from data supplied by P. Jones (Climatic Research Unit, UK). This NAO index has been calculated from the difference between the normalised sea level pressure over Gibraltar and the normalised sea level pressure over Southwest Iceland. The correlation map of the NAO and satellite SSTs during wintertime shows positive values with correlation above 0.6 in the North-Sea. These results are similar to what has been observed at the scale of the Atlantic Ocean (Wang *et al.*, 2004; Cassou, 2004). The dominance of positive NAO indexes in the last twenty years partially explains the warming trend that we have observed and the preferential warming in the North of the studied area. The mean temperatures of the surface waters for the 1903-1927 period, shown on the atlas of the English Channel published by the Conseil International pour l'Exploration de la Mer in 1933, are very close to the situation that we have calculated for the year 1986 (figure 14). It is well known that the warming has not been uniform over the last century and that a relative minimum occurred in the mid-seventies, shortly before the period considered in this study. It appears that the temperature has increased over the 1986-2006 period from a minimum of 0.5°C to a maximum of 1.5°C in the English Channel. Locally attenuated or amplified, following the atmospheric conditions of the NAO, the increase observed in the global air temperature will certainly continue to affect the SST of the English Channel in the forthcoming years. However it is statistically impossible to affirm that the warming will continue at the pace calculated in this study.

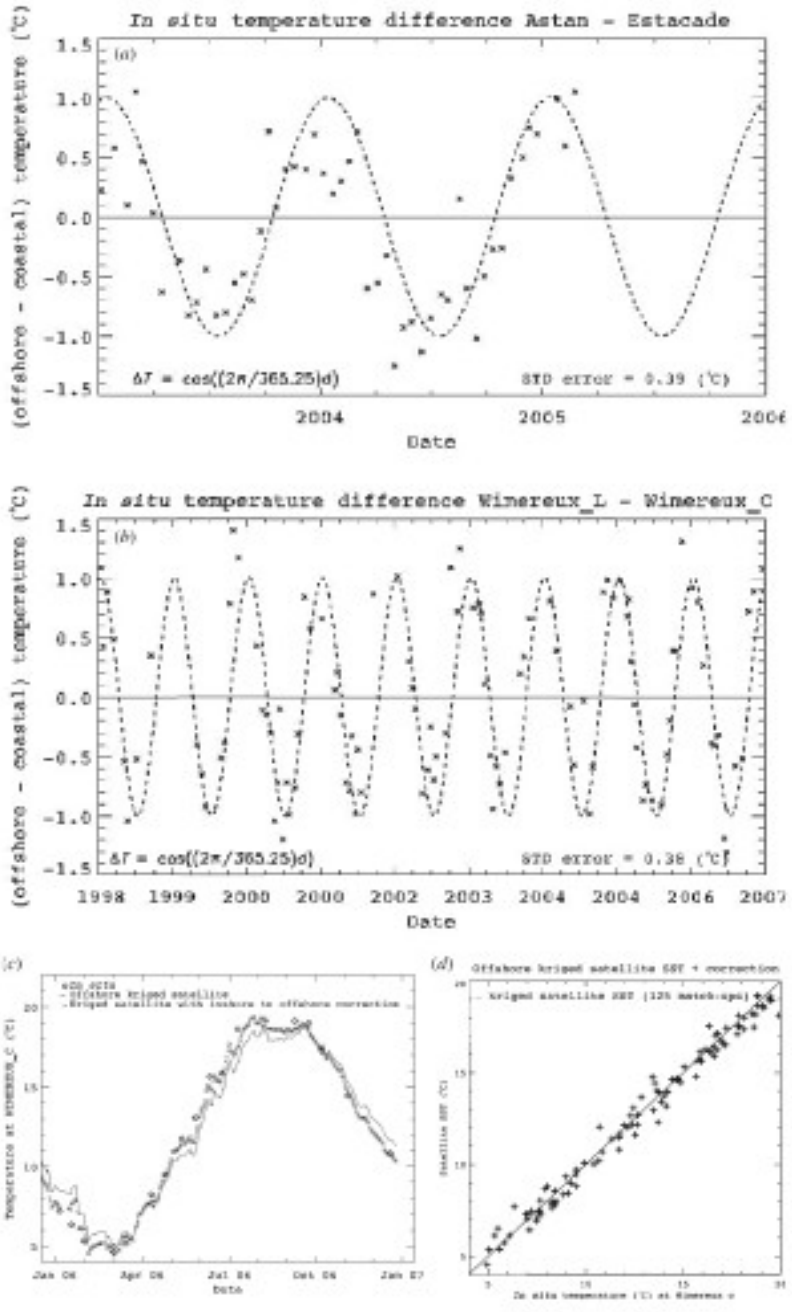

Figure 12. (*a*) *In situ* temperature differences between Wimereux_L and Wimereux_C, (*b*) Roscoff_Astan and Roscoff_Estacade, (*c*) Temperature extrapolation of the year 2006 at Wimereux_C and (*d*) Match-up scatter plot for the period 1997–2006 for the extrapolated versus *in situ* temperatures at Wimereux_C.

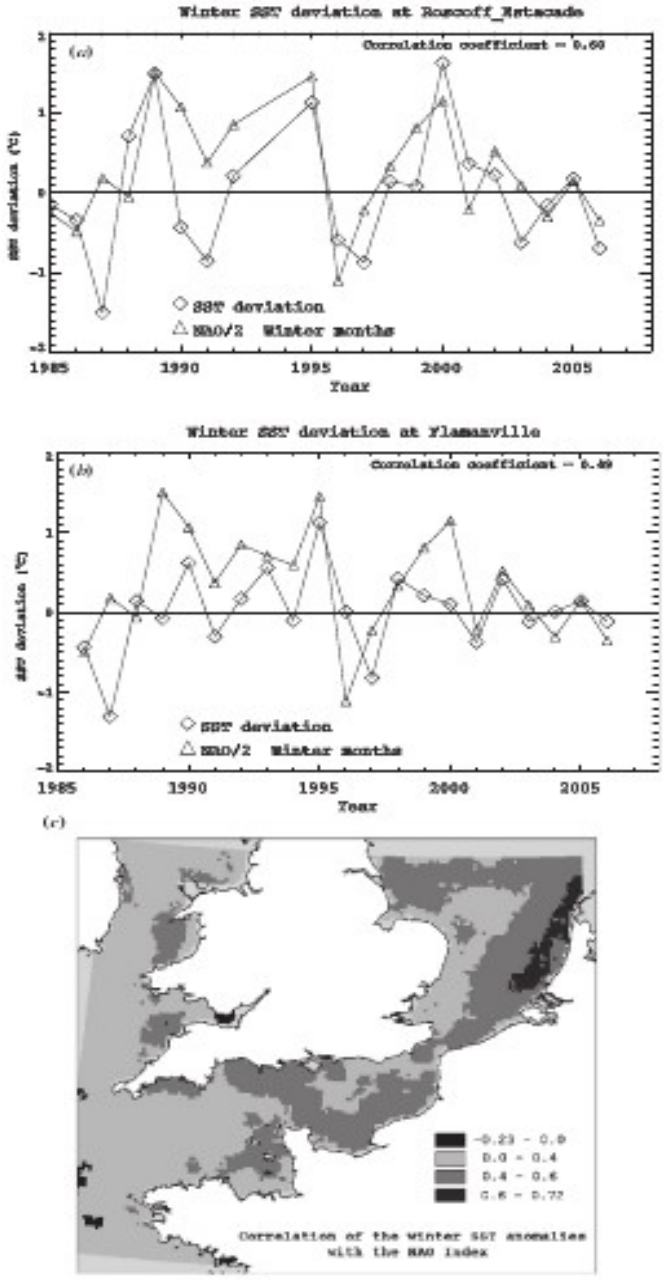

Figure 13. Time series of the SST anomaly and NAO index calculated from 15 November to 15 January at (*a*) Roscoff_Estacade and (*b*) Flamanville. (*c*) Maps of the correlation coefficient calculated using satellite SST anomalies from the model.

6. Conclusion

This work has shown that the AVHRR Pathfinder SST are quite reliable in the English Channel. The climatic interpretation of the observed trend for the 1986-2006 period is the same whether it is based on *in situ* (from only two stations) or on satellite data. These latter has the considerable advantage of providing a complete coverage on this coastal area characterized by a strong dependence of the temperature on the bathymetric structures. Despite the simplicity of the SST model, composed of a mean, a linear trend and two harmonics, most of the variance of the SST time series is well explained by the model. We have used this model as the natural underlying mean in the geostatistical hypotheses. The anomaly obtained as the difference between the SST and this model proved to be very regular and the experimental semi-variogram revealed a strong continuity. The residual effect of clouds on a small number of pixels has required a smoothing stronger than justified from the experimental semi-variogram. Nevertheless, the bias and the standard error of the estimated SST are small and comparable to the values obtained using the satellite match-ups only. The kriging of the anomalies enabled the reconstruction of daily fields of temperature at 5 km resolution. This will be of considerable interest for the operational oceanography as it will provide a complete and reliable 21-year time series at any location. As most of the stations involved in operational coastal oceanography are very coastal and cannot be observed by infra-red satellite sensors at a sufficient resolution, transfer functions between offshore and coastal stations have been defined. They open the way to a larger use of satellite data in a coastal monitoring still based on conventional networks. Although the estimated transfer function has been expressed by a simple formulation and is reliably applicable only at the studied stations, this approach is very promising. It will be a necessity in the next years to focus on the question of the variability in the vicinity of coast to extend the information of relatively low resolution space sensors to the monitoring of very coastal processes. For that purpose the incoming version 6 of Pathfinder should provide a greater number of good quality retrievals at the shore. This issue does not only concern the SST but also the other environmental parameters derived from the ocean colour technique, as chlorophyll and turbidity.

This study has been extended to the Bay of Biscay and the IBI-ROOS area (Ireland-Biscay-Iberia Regional Operating Operational System). The daily interpolated time series for 1986 to 2006 is freely available at this ftp address: ftp://www.ifremer.fr/pub/ifremer/cersat/products/gridded/sst-l4hr-AVHRR-fnd.

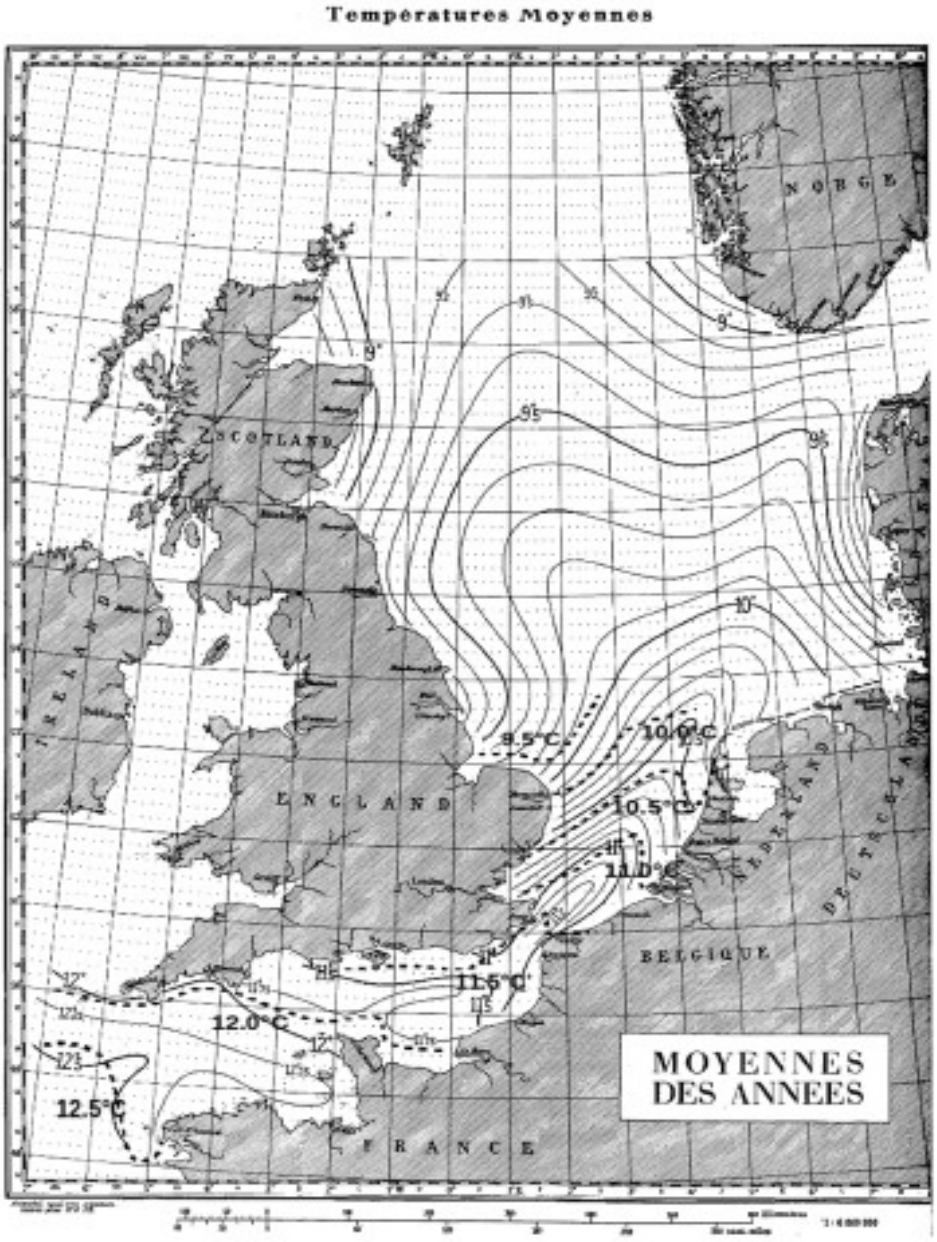

Figure 14. SST observed from *in situ* data (ICES 1933) compared to the mean temperatures of the year 1986 calculated from the SST model (dotted lines). Used with the kind permission of the International Council for the Exploration of the Sea.

Acknowledgements : We thank Luc Drévés and EDF for providing us with the Flamanville SST and CNRS/SOMLIT for the costal data of Roscoff and Wimereux. We also thank all the teams working for the AVHRR Pathfinder, NODC, RSMAS and PO.DAAC that are providing a large community with satellite data of excellent quality. This work was supported by the ECOOP (European COastal sea OPerational observing and forecasting system). ECOOP is funded by the European Commission's Sixth Framework Programme, under the priority Sustainable Development, Global Change and Ecosystems. Contract No. 36355.

References :

ARMSTRONG, E. and VAZQUEZ-CUERVO, J., 2001, A New Global Satellite-Based Sea Surface Temperature Climatology. *Geophysical Research Letters*, **28**, pp. 4199-4202.

BRETHERTON, F.P., DAVIS, R.E. and FANDRY, C.B., 1976, Technique for objective analysis and design of oceanographic experiment applied to mode-73. *Deep Sea Resarch*, **23**, pp. 559-582.

BRISSON, A., LE BORGNE, P. , MARSOUIN, A. , 2002, Results of One Year of Preoperational Production of Sea Surface Temperatures from GOES-8. *Journal of Atmospheric and Oceanic Technology*, **19**, 1638 p.

CASEY, K.S., CORNILLON, P.C., 1999, A comparison of satellite and in situ-based sea surface temperature climatologies. *Journal of Climate*, **12**, pp. 1848-1862.

CASEY, K.S., CORNILLON, P.C., 2001, Global and regional sea surface temperature trends. *Journal of Climate*, **14**, pp. 3801–3818.

CASSOU, C., 2004, Du changement climatique aux régimes de temps: l'oscillation nord-atlantique. *La météolologie*, **45**.

CASSOU C., TERRAY, L., HURRELL, J. W., and DESER, C., 2004, North Atlantic winter climate regimes: Spatial asymmetry, stationarity with time, and oceanic forcing. *Journal of Climate*, **17**, pp. 1055-1068.

CASSOU, C., DESER, C., TERRAY, L., HURRELL, J.W., AND VILLON, M., 2004, Summer Sea Surface Temperature Conditions in the North Atlantic and Their Impact upon the Atmospheric Circulation in Early Winter. *Journal of Climate*, **17**, pp. 3349-3363.

International Council for the Exploration of the Sea.
ATLAS DE TEMPERATURE ET SALINITE DE L'EAU DE SURFACE DE LA MER DU NORD ET DE LA MANCHE : PUBLIE PAR LE BUREAU DE CONSEIL, SERVICE HYDROGRAPHIQUE.
Copenhagen, 1933

DAVIS, J. C., 1986, Statistics and Data Analysis in Geology (2nd ed), John Wiley & Sons. New York, 646 p.

FAUGÈRE Y., LE BORGNE, P., and ROQUET H., 2001, Réalisation d'une climatologie mondiale de la temperature de surface de la mer. *La Météorologie*, **35**, pp. 24-35.

Gandin, L. S., 1963: *Objective Analysis of Meteorological Fields*. Hydromet Press, 242 pp..

GOHIN F. and G. LANGLOIS, 1993, Using geostatistics to merge in situ measurements and remotely-sensed observations of sea surface temperature. *International Journal of Remote Sensing*, **14**, pp. 9-19.

JOURNEL, A.G. and HUIJBREGTS, C.J., 1978, *Mining Geostatistics* (Academic Press).

KOUTSIKOPOULOS C., BEILLOIS, LEROY, C. and TAILLEFER F.,1998. Temporal Trends and spatial structures of the sea surface temperature In the Bay of Biscay. *Oceanologica Acta*, **21,** pp. 335-344.

KILPATRICK, K.A., PODESTA´ , G.P. and EVANS, R. 2001, Overview of the NOAA/NASA 535
advanced very high resolution radiometer Pathfinder algorithm for sea surface temperature
and associated match-up database. Journal of Geophysical Research, 106, pp.
9179–9197.

KRIGE, D.G, 1951, A statistical approach to some basic mine valuation problems on the Witwatersrand. *Journal of Chemistry, Metal and Mining Society of South Africa*, **52**, pp. 119-139.

MATHERON, G., 1971, The theory of regionalized variables and its applications. *Cahier du centre de Morphologie Mathémathique de Fontainbleau-France*, **5**, 211 p.

MCCLAIN, E. P., PICHEL, W. G. and WALTON, C. C., 1985, Comparative performance of AVHRR-based multichannel sea surface temperatures. *Journal of Geophysical Research*, **90**, pp. 11587–11601.

MESIAS M., BISAGNI J., BRUNER A., 2007, A high resolution satellite-derived sea surface temperature climatology for the Western North Atlantic Ocean. *Continental Shelf Research*, **27**, pp. 191-207.

REYNOLDS R. W., 2002, An Improved In Situ and Satellite SST Analysis for Climate. *Journal of Climate*, **15**, pp.1609-1625.

REYNOLDS, R., SMITH, T., 1994, Improved global sea surface temperature analyses using optimal interpolation. *Journal of Climate*, **7**, pp. 929–948.

REYNOLDS, R., SMITH, T., 1995, A high-resolution global sea surface temperature climatology. *Journal of Climate*, **8**, pp. 1571–1583.

SCHEFFER, M., CARPENTER, S., FOLEY, J.A., FOLKE, C., WALKER, B., 2001, Catastrophic shifts in ecosystems. *Nature*, **413**, pp. 591–596.

SHERMAN, K., SKJOLDAL, H.R., 2002, *Large Marine Ecosystems of the North Atlantic: Changing States and Sustainability* (Elsevier).

STRONG, A.E., KEARNS, E.J., and GJOVIG, K.K., 2000, Sea surface temperature Signals from satellite – An update. *Geophysical Research Letters*, **27**, pp. 1667-1670.

VASQUEZ, J., PERRY, K., KILPATRICK, K., 1998, NOAA/NASA AVHRR Oceans Pathfinder sea surface temperatures data user's reference manual, Version 4.0. JPL Technical Report D-14070, available at: http://podaac.jpl.nasa.gov/.

WANG, W., ANDERSON, B.T., KAUFMANN, R.K., and MYNENI, R.B., 2004, The Relation between the North Atlantic Oscillation and SSTs in the North Atlantic Basin. *Journal of Climate*, **17**, pp. 4752-4759.

WALTON, C. C., PICHEL W. G., SAPPER F. J., and MAY, D. A., 1998, The development and operational application of non linear algorithms for the measurement of sea surface temperatures with NOAA polar-orbiting environmental satellites. *Journal of Geophysical Research*, **103**, pp. 27999–28012.